Stagnation-Point Flow and Heat Transfer of a Casson Fluid towards a Stretching Sheet

Meraj Mustafa[a], Tasawar Hayat[b,c], Ioan Pop[d], and Awatif Hendi[c]

[a] Research Centre for Modeling and Simulation (RCMS), National University of Sciences and Technology (NUST), Sector H-12, Islamabad 44000, Pakistan
[b] Department of Mathematics, Quaid-I-Azam University 45320, Islamabad 44000, Pakistan
[c] Department of Physics, Faculty of Science, King Saud University, P. O. Box 1846, Riyadh 11321, Saudi Arabia
[d] Faculty of Mathematics, University of Cluj, R-3400 Cluj, Romania

Reprint requests to M. M.; Tel.: + 92 51 90855733, E-mail: meraj_mm@hotmail.com

Z. Naturforsch. **67a,** 70 – 76 (2012) / DOI: 10.5560/ZNA.2011-0057
Received June 6, 2011 / revised October 2, 2011

This article reports the flow of a Casson fluid in the region of stagnation-point towards a stretching sheet. The characteristics of heat transfer with viscous dissipation are also analyzed. The partial differential equations representing the flow and heat transfer of the Casson fluid are reduced to ordinary differential equations through suitable transformations. The flow is therefore governed by the Casson fluid parameter β, the ratio of the free stream velocity to the velocity of the stretching sheet a/c, the Prandtl number Pr, and the Eckert number Ec. The analytic solutions in the whole spatial domain have been computed by the homotopy analysis method (HAM). The dimensionless expressions for the skin friction coefficient and the local Nusselt number have been calculated and discussed.

Key words: Casson Fluid; Viscous Dissipation; Heat Transfer; Analytic Solutions.

1. Introduction

The boundary-layer theory is among the most successful idealization in the history of Newtonian fluid mechanics [1]. With the help of this theory, many fluid flows and heat transfer problems have been very successfully mathematically modelled, with results that agree very well with experimental observations. However, many fluids of industrial importance are non-Newtonian and an extension of the theory of Newtonian fluids to the theory of such fluids has proved to be not so straightforward (see, for example, [2 – 6]). It is now generally recognized that, in real industrial applications, non-Newtonian fluids are more appropriate than Newtonian fluids. These fluids have wide-ranging industrial applications, for example, in the design of thrust bearings and radial diffusers, drag reduction, transpiration cooling, thermal oil recovery, etc. In certain polymer processing applications, one deals with the flow of a second-order (viscoelastic) fluid over a stretching surface. Such fluids are referred to as fluids of the differential type, that is, fluids whose stress is determined by the Rivlin–Ericksen tensors [7], or fluids of the rate type, such as the Oldroyd-B fluid [8]. Polymers mixed in Newtonian solvents and polymer melts, such as high-viscosity silicone oils or molten plastics, are examples of such fluids. Numerous models have been suggested for non-Newtonian fluids, with their constitutive equations varying greatly in complexity. Some authors have studied the Casson fluid for the flow between two rotating cylinders [9] and for the steady and oscillatory blood flow [10].

The problem of the boundary-layer flow of an incompressible viscous fluid (Newtonian fluids) near the stagnation point on a stretching sheet has an important bearing on several technological processes. In fact, this problem belongs to a very large class of stretching problems, which are very well described physically and very well documented in the literature (see, for example, [11 – 19], etc.). An example of a stretching surface is a polymer sheet of filament extruding continuously from a die or a long thread travelling between a feed roll and a wind-up roll. Another example that belongs to this class of problems is the cooling of a large metallic plate in a bath, which may be an electrolyte. In all of these cases, a study of the

flow field and heat transfer can be of significant importance since the quality of the final product depends to a large extent on the skin friction coefficient and the surface heat transfer rate. The present paper aims to study the steady boundary-layer flow of a Casson fluid near the stagnation-point on a stretching surface using the homotopy analysis method (HAM) which has been successfully applied to various interesting problems [20 – 29]. The novel results presented in this study demonstrate the existence of similar solutions of the boundary-layer equations for a class of general non-Newtonian fluids for a stretching surface. For solutions being similar, the problem is reduced to the solution of a set of two nonlinear ordinary differential equations that are solved analytically using HAM for a range of values of the governing parameters. Results are compared with those from the open literature for some particular values of the governing parameters and it is found that they are in a very good agreement.

2. Basic Equations

Consider the steady two-dimensional flow of a Casson fluid near the stagnation-point on a heated stretching surface coinciding with the plane $y = 0$, the flow being confined to $y > 0$, where y is the coordinate normal to the surface. Two equal and opposite forces are applied along the x-axis (measured along the surface) so that the surface is stretched keeping the origin fixed. It is assumed that the velocity distribution far from the surface (potential flow) is given by $u_e(x) = ax$ and $v_e(y) = -ay$, while the velocity of the stretching surface is $u_w(x) = cx$ where a and c are positive constants. It is also assumed that the temperature of the plate is $T_w(x)$, while the uniform temperature of the ambient fluid is T_∞. We assume that the rheological equation of state for an isotropic and incompressible flow of a Casson fluid can be written as [30]

$$\tau_{ij} = \begin{cases} 2\left(\mu_B + p_y/\sqrt{2\pi}\right) e_{ij}, & \pi > \pi_c, \\ 2\left(\mu_B + p_y/\sqrt{2\pi_c}\right) e_{ij}, & \pi < \pi_c, \end{cases} \tag{1}$$

where $\pi = e_{ij}e_{ij}$ and e_{ij} is the (i, j)th component of the deformation rate, π is the product of the component of deformation rate with itself, π_c is a critical value of this product based on the non-Newtonian model, μ_B is the plastic dynamic viscosity of the non-Newtonian fluid, and p_y is the yield stress of the fluid. Under these conditions along with the assumption that the viscous dissipation term in the energy equation is taken into consideration, the boundary layer equations which govern this problem are

$$\frac{\partial u}{\partial x} + \frac{\partial v}{\partial y} = 0, \tag{2}$$

$$u\frac{\partial u}{\partial x} + v\frac{\partial u}{\partial y} = u_e\frac{\mathrm{d}u_e}{\mathrm{d}x} + \nu\left(1 + 1/\beta\right)\frac{\partial^2 u}{\partial y^2}, \tag{3}$$

$$u\frac{\partial T}{\partial x} + v\frac{\partial T}{\partial y} = \alpha\frac{\partial^2 T}{\partial y^2} + \frac{\nu}{C_p}\left(1 + 1/\beta\right)\left(\frac{\partial u}{\partial y}\right)^2, \tag{4}$$

subject to the boundary conditions

$$\begin{aligned} &u = u_w(x) = cx, \;\; v = 0, \;\; T = T_w(x) = T_\infty + bx^2 \\ &\qquad \text{at } y = 0, \\ &u \to u_e(x) = ax, \;\; T \to T_\infty \;\; \text{as} \;\; y \to \infty, \end{aligned} \tag{5}$$

where b is a positive constant, $\beta = \mu_B\sqrt{2\pi_c}/p_y$ is the non-Newtonian (Casson) parameter, α is the thermal diffusivity, ν is the kinematic viscosity, and C_p is the specific heat.

We introduce the following similarity variables:

$$\psi = x\sqrt{c\nu}f(\eta), \;\; \theta(\eta) = \frac{T - T_\infty}{T_w - T_\infty}, \;\; \eta = \sqrt{\frac{c}{\nu}}y, \tag{6}$$

where ψ is the stream function which is defined in the usual way as $u = \partial\psi/\partial y$ and $v = -\partial\psi/\partial x$. Substituting (6) into (3) and (4), the set of ordinary differential equations results in

$$\left(1 + 1/\beta\right)f''' + ff'' - f'^2 + \frac{a^2}{c^2} = 0, \tag{7}$$

$$\frac{1}{\mathrm{Pr}}\theta'' + f\theta' - 2f'\theta + \left(1 + 1/\beta\right)\mathrm{Ec}\,f''^2 = 0, \tag{8}$$

and the boundary conditions in (5) become

$$\begin{aligned} &f(0) = 0, \;\; f'(0) = 1, \;\; \theta(0) = 1, \\ &f'(\infty) \to \frac{a}{c}, \;\; \theta(\infty) \to 0. \end{aligned} \tag{9}$$

Here $\mathrm{Pr} = \nu/\alpha$ is the Prandtl number, $\mathrm{Ec} = u_w^2/\left[C_p\left(T_w - T_\infty\right)\right]$ is the constant Eckert number, and the prime denotes differentiation with respect to η. It is worth mentioning that for a regular viscous fluid ($\beta \to \infty$), (7) and (8) reduce to (12) and (20) from the paper by Mahapatra and Gupta [14].

The physical quantities of interest are the skin friction coefficient C_f and the local Nusselt number Nu_x, which are defined as

$$C_\mathrm{f} = \frac{\tau_w}{\rho u_w^2(x)}, \;\; \mathrm{Nu}_x = \frac{xq_w}{k(T_w - T_\infty)}, \tag{10}$$

where τ_w is the skin friction or shear stress along the stretching surface and q_w is the heat flux from the surface, which are given by

$$\tau_w = \left(\mu_\beta + \frac{p_y}{\sqrt{2\pi_c}}\right)\left(\frac{\partial u}{\partial y}\right)_{y=0}, \qquad q_w = -k\left(\frac{\partial T}{\partial y}\right)_{y=0}. \tag{11}$$

Using (6), we get

$$\mathrm{Re}_x^{1/2} C_f = (1+1/\beta) f''(0), \qquad \mathrm{Nu}_x/\mathrm{Re}_x^{1/2} = -\theta'(0), \tag{12}$$

where $\mathrm{Re}_x = u_w(x)x/\nu$ is the local Reynolds number.

3. Homotopy Analysis Solutions

Following the rule of solution expressions for f and θ and the boundary conditions (9) we select the initial guesses for f and θ in the forms

$$f_0(\eta) = \frac{a}{c}\eta + (1-A)(1-\exp(-\eta)), \qquad \theta_0(\eta) = \exp(-\eta), \tag{13}$$

and the auxiliary linear operators are expressed as

$$\mathcal{L}_f = \frac{\mathrm{d}^3 f}{\mathrm{d}\eta^3} - \frac{\mathrm{d}f}{\mathrm{d}\eta}, \quad \mathcal{L}_\theta = \frac{\mathrm{d}^2\theta}{\mathrm{d}\eta^2} - \theta, \tag{14}$$

with

$$\mathcal{L}_f\left[C_1 + C_2\exp(\eta) + C_3\exp(-\eta)\right] = 0, \qquad \mathcal{L}_\theta\left[C_4\exp(\eta) + C_5\exp(-\eta)\right] = 0, \tag{15}$$

and C_i $(i = 1-5)$ are the arbitrary constants. Let $p \in [0,1]$ indicate the embedding parameter and $\hbar_f$ and $\hbar_\theta$ the nonzero auxiliary parameters. The relevant problems at the zeroth and mth-order problems are constructed as

$$(1-p)\mathcal{L}_f[\hat{f}(\eta,p) - f_0(\eta)] = p\hbar_f \mathcal{N}_f\left[\hat{f}(\eta,p), \hat{\theta}(\eta,p)\right], \tag{16}$$

$$(1-p)\mathcal{L}_\theta[\hat{\theta}(\eta,p) - \theta_0(\eta)] = p\hbar_\theta \mathcal{N}_\theta\left[\hat{f}(\eta,p), \hat{\theta}(\eta,p)\right], \tag{17}$$

$$\hat{f}(\eta;p)\big|_{\eta=0} = 0, \quad \left.\frac{\partial \hat{f}(\eta;p)}{\partial\eta}\right|_{\eta=0} = 1, \quad \left.\frac{\partial \hat{f}(\eta;p)}{\partial\eta}\right|_{\eta=\infty} = \frac{a}{c}, \tag{18}$$

$$\hat{\theta}(\eta;p)\big|_{\eta=0} = 1, \quad \hat{\theta}(\eta;p)\big|_{\eta=\infty} = 0, \tag{19}$$

$$\mathcal{L}_f\left[f_m(\eta) - \chi_m f_{m-1}(\eta)\right] = \hbar_f \mathcal{R}_m^f(\eta), \tag{20}$$

$$\mathcal{L}_\theta\left[\theta_m(\eta) - \chi_m \theta_{m-1}(\eta)\right] = \hbar_\theta \mathcal{R}_m^\theta(\eta), \tag{21}$$

$$f_m(0) = 0, \quad f_m'(0) = 0, \quad f_m'(\infty) = 0, \qquad \theta_m(0) = 0, \quad \theta_m(\infty) = 0, \tag{22}$$

$$\mathcal{N}_f\left[\hat{f}(\eta;p), \hat{\theta}(\eta;p)\right] = (1+1/\beta)\frac{\partial^3 \hat{f}(\eta,p)}{\partial\eta^3} + \hat{f}(\eta,p)\frac{\partial^2 \hat{f}(\eta,p)}{\partial\eta^2} - \left(\frac{\partial \hat{f}(\eta,p)}{\partial\eta}\right)^2 + \frac{a^2}{c^2}, \tag{23}$$

$$\mathcal{N}_\theta\left[\hat{f}(\eta;p), \hat{\theta}(\eta;p)\right] = \frac{1}{\mathrm{Pr}}\frac{\partial^2 \hat{\theta}(\eta,p)}{\partial\eta^2} + \hat{f}(\eta,p)\frac{\partial \hat{\theta}(\eta,p)}{\partial\eta} - 2\frac{\partial \hat{f}(\eta,p)}{\partial\eta}\hat{\theta}(\eta,p) + \mathrm{Ec}\,(1+1/\beta)\left(\frac{\partial^2 \hat{f}(\eta,p)}{\partial\eta^2}\right)^2, \tag{24}$$

$$\mathcal{R}_m^f(\eta) = (1+1/\beta) f_{m-1}''' + \sum_{k=0}^{m-1}\left[f_{m-1-k} f_k'' - f_{m-1-k}' f_k'\right] + \frac{a^2}{c^2}(1-\chi_m), \tag{25}$$

$$\mathcal{R}_m^\theta(\eta) = \frac{1}{\mathrm{Pr}}\theta_{m-1}'' + \sum_{k=0}^{m-1}\left[f_{m-1-k}\theta_k' - 2 f_{m-1-k}'\theta_k\right] + \mathrm{Ec}\sum_{k=0}^{m-1} f_{m-1-k}'' f_k'', \tag{26}$$

$$\chi_m = \begin{cases} 0, & m \le 1, \\ 1, & m > 1, \end{cases} \tag{27}$$

where for $p = 0$ and $p = 1$, we have

$$\hat{f}(\eta;0) = f_0(\eta), \quad \hat{f}(\eta;1) = f(\eta), \tag{28}$$

$$\hat{\theta}(\eta;0) = \theta_0(\eta), \quad \hat{\theta}(\eta;1) = \theta(\eta). \tag{29}$$

Employing Taylor's theorem, we can write

$$\hat{f}(\eta;p) = f_0(\eta) + \sum_{m=1}^{\infty} f_m(\eta) p^m, \qquad f_m(\eta) = \frac{1}{m!}\left.\frac{\partial^m f(\eta;p)}{\partial\eta^m}\right|_{p=0}, \tag{30}$$

$$\hat{\theta}(\eta;p) = \theta_0(\eta) + \sum_{m=1}^{\infty} \theta_m(\eta) p^m, \qquad \theta_m(\eta) = \frac{1}{m!}\left.\frac{\partial^m \theta(\eta;p)}{\partial\eta^m}\right|_{p=0}, \tag{31}$$

in which the auxiliary parameters are selected in such a way that the series (31) and (32) converge at $p = 1$ and hence

$$f(\eta) = f_0(\eta) + \sum_{m=1}^{\infty} f_m(\eta), \tag{32}$$

$$\theta(\eta) = \theta_0(\eta) + \sum_{m=1}^{\infty} \theta_m(\eta). \tag{33}$$

The general solutions of (20)–(22) are

$$f_m(\eta) = f_m^*(\eta) + C_1 + C_2 \exp(\eta) + C_3 \exp(-\eta), \tag{34}$$

$$\theta_m(\eta) = \theta_m^*(\eta) + C_4 \exp(\eta) + C_5 \exp(-\eta), \tag{35}$$

where $f_m^*(\eta)$ and $\theta_m^*(\eta)$ denote the special solutions and

$$C_2 = C_4 = 0,$$
$$C_1 = -C_3 - f_m^*(0), \; C_3 = \left.\frac{\partial f^*(\eta)}{\partial \eta}\right|_{\eta=0}, \tag{36}$$
$$C_5 = -\theta_m^*(0).$$

Equations (20)–(22) have been solved by utilizing the symbolic software Mathematica for $m = 1, 2, 3, \ldots$.

4. Analysis of the Results

4.1. Convergence of the Homotopy Solutions

The auxiliary parameters appearing in (20) and (21) can easily adjust and control the convergence of the derived expressions. To select appropriate values of these parameters, we display the so-called $\hbar_f$- and $\hbar_\theta$-curves at 15th-order of approximations for various values of stretching ratio a/c. The admissible range of $\hbar_f$ and $\hbar_\theta$ can be obtained from the line segment parallel to the $\hbar_f$-, $\hbar_\theta$-axis in Figures 1 and 2 [21]. For $a/c = 0.2$ and $\beta = 1.0$, the ranges for $\hbar_f$ and $\hbar_\theta$ are $-0.8 \leq \hbar_f \leq -0.3$ and $-0.8 \leq \hbar_\theta \leq -0.4$, respectively. It is observed that the range for $\hbar_f$ shifts towards the right hand side with an increase in a/c (Fig. 1). From Figure 2 it is seen that the range for $\hbar_\theta$ slightly shrinks for large values of a/c. In order to see the accuracy of the present results, we display the three-dimensional $\hbar_f, \hbar_\theta \sim \eta$ curves for the residual error at 15th-order of approximations. Here we can easily determine the values of $\hbar_f$ and $\hbar_\theta$ which are giving minimum error. It is evident from Figures 3 and 4 that the obtained results are accurate up to six decimal places for all the values of the similarity variable η when we select $\hbar_f = \hbar_\theta = -0.6$.

4.2. Results and Discussion

In order to analyze the behaviours of various parameters on the velocity and temperature fields, Figures 5–9 are sketched. Since the obtained series solutions converge at 15th-order of approximations, these figures are plotted for 15th-order HAM solution. The effect of stretching ratio a/c on the velocity field f' is observed in Figure 5. For small values of a/c ($0 \leq a/c < 1$) the velocity and boundary layer thickness increase with an increase in a/c. An increase in the velocity follows from the fact that gradual increase in a/c increases the free stream velocity which results in the

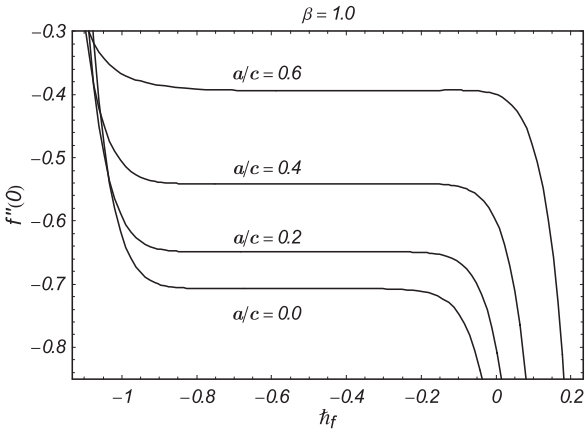

Fig. 1. $\hbar$-curve for the function f.

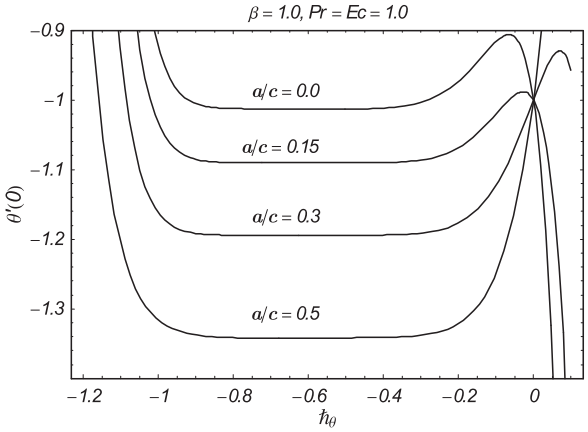

Fig. 2. $\hbar$-curve for the function θ.

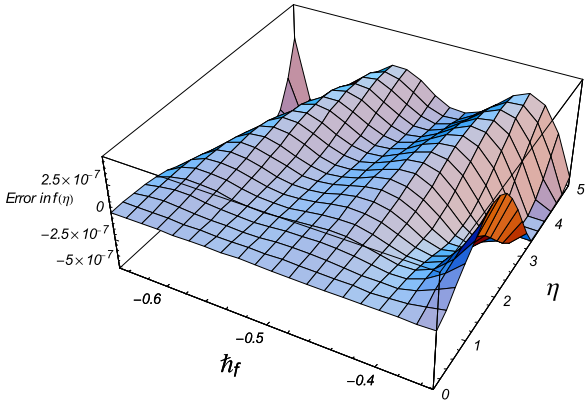

Fig. 3 (colour online). Residual error for the function f.

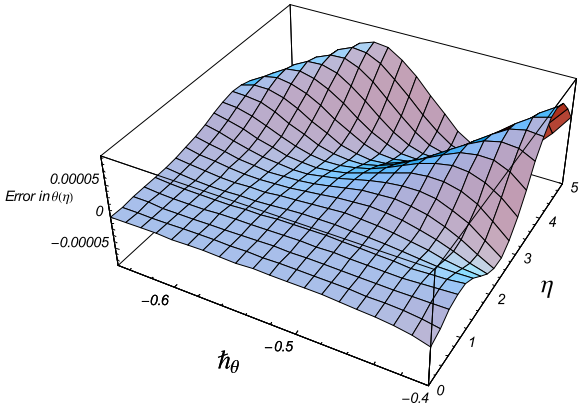

Fig. 4 (colour online). Residual error for the function θ.

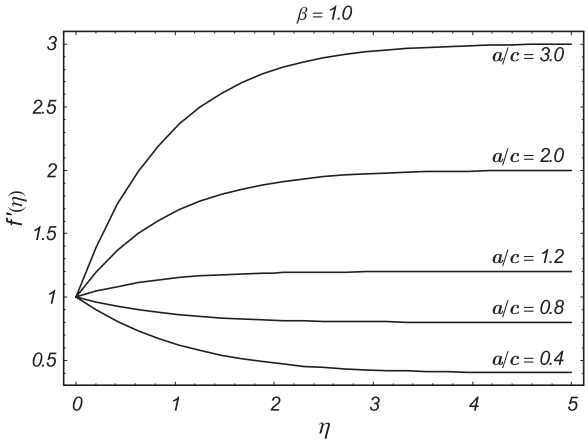

Fig. 5. Influence of a/c on f'.

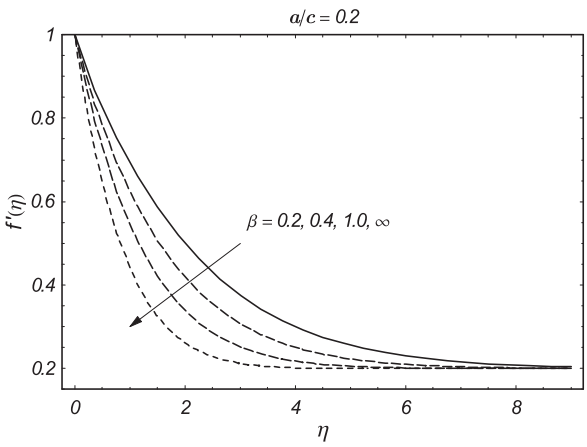

Fig. 6. Influence of β on f'.

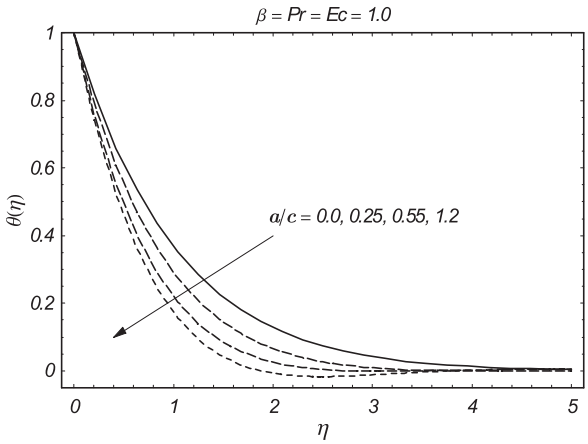

Fig. 7. Influence of a/c on θ.

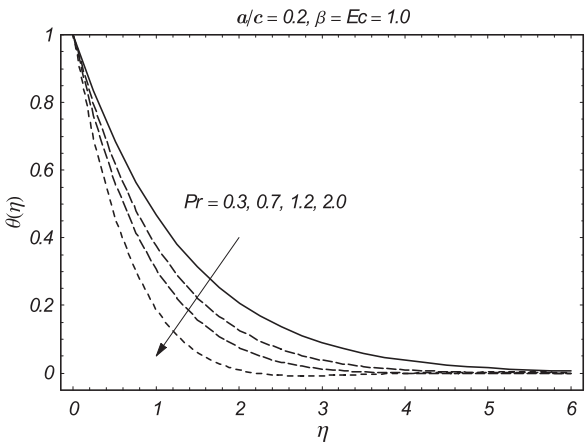

Fig. 8. Influence of Pr on θ.

increase in the velocity. For large values of a/c, the velocity increases and the boundary layer thickness decreases with the increasing values of a/c. The influence of non-Newtonian (Casson) parameter β on the velocity field is depicted in Figure 6. An increase in β corresponds to a decrease in the velocity and the

boundary layer thickness for fixed value of $a/c(=0.2)$. Thus it is quite obvious that the magnitude of velocity is greater in the case of the Casson fluid when compared with the viscous fluid. To observe the influences of embedding parameters such as stretching ratio a/c, Prandtl number Pr, and Eckert number Ec on the temperature θ, Figures 7–9 are displayed. The consequences of an increase in a/c on the temperature are seen in Figure 7. An increase in a/c results in the decrease of temperature and the thermal boundary layer thickness. Thus the stronger free stream velocity causes a reduction in the temperature and the thermal boundary layer thickness. The outcome of an increase in the Prandtl number Pr is captured in Figure 8. From the definition of Pr it is obvious that a rapid increase in Pr decreases the thermal conductivity which tends to decrease the temperature and the thermal boundary layer thickness. This observation can be easily visualized in Figure 8. Furthermore, it is noticed that the temperature profiles show an appreciable increase for small values of Pr. An enhancement in the Eckert number Ec results in the increase in the temperature θ. This change is quite siginificant for large values of Ec (see Fig. 9).

Table 1 is prepared to visualize the convergence rate of the obtained series solutions. It is noticed that the series solutions converge at only 15th-order of approximations. The present results are compared with those of Mahapatra and Gupta [14] and Ishak et al. [20] for the case of viscous fluid. The numerical results for the skin friction coefficient were found to be in excellent agreement with the current results. In Tables 3 and 4, the numerical values of skin friction coefficient and local Nusselt number are obtained for different values of parameters. The magnitude of the skin friction coefficient is a decreasing function of β and a/c. The large values of Ec decrease the magnitude of local Nusselt

Table 1. Convergence of series solutions for different order of approximations when $a/c = 0.2$, $\beta = 1.0$, $\mathrm{Pr} = \mathrm{Ec} = 1.0$, and $\hbar_f = \hbar_\theta = -0.6$.

Order of approximations	$-f''(0)$	$-\theta'(0)$
1	0.604000	0.993000
5	0.648635	1.122912
10	0.649206	1.123112
15	0.649120	1.123090
20	0.649120	1.123100
25	0.649120	1.123100
35	0.649120	1.123100
40	0.649120	1.123100

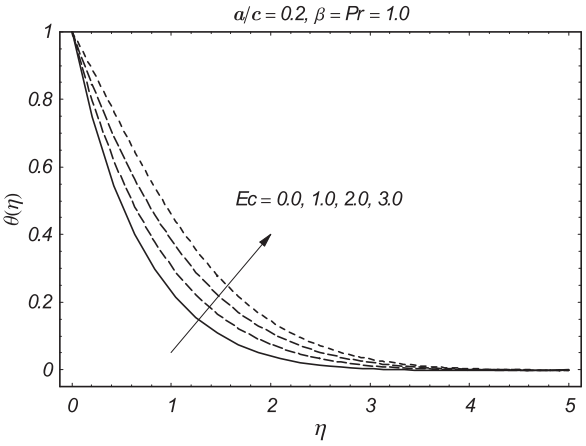

Fig. 9. Influence of Ec on θ.

Table 2. Comparison of values of $f''(0)$ with those of Mahapatra and Gupta [14] and Ishak et al. [20] for various values of a/c when $\beta \to \infty$, $\hbar_f = \hbar_\theta = -0.6$.

a/c	Present	Mahapatra and Gupta [14]	Ishak et al. [20]
0.01	−0.99802	–	−0.9980
0.10	−0.96939	−0.9694	−0.9694
0.20	−0.91807	−0.9181	−0.9181
0.50	−0.66735	−0.6673	−0.6673
2.00	2.01757	2.0175	2.0175
3.00	4.72964	4.7294	4.7294

Table 3. Values of skin friction coefficient and local Nusselt number for various values of β and a/c when $\mathrm{Pr} = \mathrm{Ec} = 1.0$ and $\hbar_f = \hbar_\theta = -0.6$.

β	a/c	$\mathrm{Re}_x^{1/2} C_f$	$\mathrm{Re}_x^{-1/2} \mathrm{Nu}_x$
0.7	0.2	−1.430767	−1.120981
1.0		−1.298400	−1.123109
1.5		−1.185271	−1.123877
∞		−0.918107	−1.119034
1.0	0.0	−1.414214	−1.012816
	0.1	−1.370919	−1.059920
	0.3	−1.201263	−1.194360
	0.5	−1.082333	−1.268512

Table 4. Values of local Nusselt number for various values of Pr and Ec when $\beta = 1.0$, $a/c = 0.2$, and $\hbar_f = \hbar_\theta = -0.6$.

Pr	Ec	$\mathrm{Re}_x^{-1/2} \mathrm{Nu}_x$
0.8	1.0	−1.005229
1.2		−1.228155
1.5		−1.368437
2.0		−1.570291
1.0	0.5	−1.280454
	0.8	−1.186041
	1.5	−0.965744
	2.0	−0.808389

number whereas the Nusselt number show an appreciable increase with the increasing values of β, a/c, and Pr.

5. Conclusions

The flow and heat transfer of a non-Newtonian (Casson) fluid is investigated about a stagnation-point on a stretching sheet. The resulting problems have been computed by the homotopy analysis method (HAM). The main points of this study are:

- It is obvious from Table 1 that the series solutions converge at only 15th-order of approximations up to six decimal places.
- The magnitudes of velocity and skin friction coefficient are greater in case of the Casson fluid when compared with the viscous fluid.
- Temperature and thermal boundary layer thickness are decreasing functions of the non-Newtonian (Casson) parameter.
- The influence of Prandtl number Pr and Casson fluid parameter β on the temperature is similar in a qualitative sense.
- The effect of Eckert number Ec is to increase the temperature and the thermal boundary layer thickness.
- The present results in the limiting case ($\beta \to \infty$) are found in excellent agreement with those of Mahapatra and Gupta [14] and Ishak et al. [20].

Acknowledgement

Second author as a Visiting Professor appreciates the support of Global Research Network for Computational Mathematics and King Saud University for this research.

[1] H. Schlichting and K. Gersten, Boundary Layer Theory, Springer, Berlin 2000.
[2] A. H. P. Skelland, Non-Newtonian Flow and Heat Transfer, John Wiley & Sons, New York 1966.
[3] M. M. Denn, Chem. Eng. Sci. **22**, 395 (1967).
[4] K. R. Rajagopal, A. S. Gupta, and A. S. Wineman, Appl. Sci. Eng. Lett. **18**, 875 (1980).
[5] R. B. Bird, R. C. Armstrong, and O. Hassager, Dynamics of Polymer Liquids (2nd edition), Wiley, New York 1987.
[6] J. C. Slattery, Advanced Transport Phenomena, Cambridge University Press, Cambridge 1999.
[7] R. S. Rivlin and J. L. Ericksen, J. Rational Mech. Anal. **4**, 323 (1955).
[8] J. G. Oldroyd, Proc. R. Soc. London A **200**, 523 (1950).
[9] N. T. M. Eldabe and M. G. E. Salwa, J. Phys. Soc. Japan **64**, 4164 (1995).
[10] J. Boyd, J. M. Buick, and S. Green, Phys. Fluids **19**, 093103 (2007).
[11] T. C. Chiam, J. Phys. Soc. Japan **63**, 2443 (1994).
[12] T. C. Chiam, Int. Commun. Heat Mass Transfer **23**, 239 (1996).
[13] T. R. Mahapatra and A. S. Gupta, Acta Mech. **152**, 191 (2001).
[14] T. R. Mahapatra and A. S. Gupta, Heat Mass Transfer **38**, 517 (2002).
[15] T. R. Mahapatra and A. S. Gupta, The Canadian J. Chem. Eng. **81**, 258 (2003).
[16] C. Y. Wang, J. Appl. Math. Phys. (ZAMP) **54**, 184 (2003).
[17] C. Y. Wang, Chem. Eng. Sci. **61**, 7668 (2006).
[18] T. R. Mahapatra, S. K. Nandy, and A. S. Gupta, Int. J. Nonlin. Mech. **44**, 124 (2009).
[19] J. Javed, Z. Abbas, T. Hayat, and S. Asghar, ASME. J. Heat Transfer **131**, 094506-1 (2009).
[20] A. Ishak, R. Nazar, N. Amin, D. Filip, and I. Pop, Malaysian J. Math. Sci. **2**, 217 (2007).
[21] S. J. Liao, Commun. Nonlin. Sci. Num. Simul. **14**, 983 (2009).
[22] H. Xu, S. J. Liao, and X. C. You, Commun. Nonlin. Sci. Num. Simul. **14**, 1152 (2009).
[23] S. Abbasbandy, Nonlin. Anal.: Real World Appl. **11**, 307 (2010).
[24] S. Abbasbandy and A. Shirzadi, Commun. Nonlin. Sci. Num. Simul. **16**, 112 (2011).
[25] I. Hashim, O. Abdulaziz, and S. Momani, Commun. Nonlin. Sci. Num. Simul. **14**, 674 (2009).
[26] A. S. Bataineh, M. S. M. Noorani, and I. Hashim, Commun. Nonlin. Sci. Num. Simul. **14**, 1121 (2009).
[27] T. Hayat, K. Maqbool, and S. Asghar, Num. Methods Part. Diff. Eq. **26**, 501 (2010).
[28] T. Hayat, M. Mustafa, and I. Pop, Commun. Nonlin. Sci. Numer. Simul. **15**, 1183 (2010).
[29] T. Hayat, M. Mustafa, and S. Asghar, Nonlin. Anal.: Real World Appl. **11**, 3186 (2010).
[30] M. Nakamura and T. Sawada, ASME J. Biomech. Eng. **110**, 137 (1988).